Research paper

'Pressure fatigue': the influence of sap pressure cycles on cavitation vulnerability in *Acer negundo*

Toshihiro Umebayashi[1,2,5], John S. Sperry[1], Duncan D. Smith [1,3] and David M. Love[1,4]

[1]School of Biological Sciences, University of Utah, 257 S 1400E, Salt Lake City, UT 84112, USA; [2]Present address: Research Faculty of Agriculture, Hokkaido University, Sapporo, Japan; [3]Present address: Department of Botany, University of Wisconsin – Madison, Madison, WI, USA; [4]Present address: Warnell School of Forestry and Natural Resources, Athens, GA, USA; [5]Corresponding author (toshiumebayashi@gmail.com)

Vulnerability-to-cavitation curves (VCs) can vary within a tree crown in relation to position or branch age. We tested the hypothesis that VC variation can arise from differential susceptibility to the number of diurnal sap pressure cycles experienced. We designed a method to distinguish between effects of cycling vs exposure time to negative pressure, and tested the influence of sap pressure cycles on cavitation vulnerability between upper and lower branches in *Acer negundo* L. trees using static and flow centrifuge, and air-injection methods. Branches from the upper crown had greater hydraulic conductivity and were more resistant to cavitation than branches from the lower crown. Upper branches also showed little change after exposure to 10 or 20 pressure cycles between −0.5 MPa and −2.0 MPa. Lower branches, however, showed a marked increase in vulnerability to cavitation after pressure-cycling. This result suggests that 'cavitation fatigue' can occur without the actual induction (and reversal) of cavitation as documented previously, but simply from the cycling of pressures in the sub-cavitation range. This 'pressure fatigue' may explain age-related shifts in VCs that could eventually induce dieback in suppressed branches or trees. Pressure fatigue may help explain developmental variation in hydraulic capacity of branches within individuals.

Keywords: *Acer negundo*, branch dieback, cavitation, cycle effect, vulnerability curve, water relation.

Introduction

In plants, water moves through xylem conduits (tracheids and vessels) from roots to leaves under negative pressure. Many researchers have investigated how loss of hydraulic conductivity in xylem (K_h) in plant organs relates to water stress and/or freeze–thaw cycles (Cochard and Tyree 1990, Sperry and Sullivan 1992, Davis et al. 1999). The native percentage loss of K_h (PLC) fluctuates throughout the year depending on species and environmental conditions (Sperry et al. 1994, Alder et al. 1996), and exceptionally high PLC during the growing season has been associated with mortality in some species (Barigah et al. 2013, Li et al. 2016, Umebayashi et al. 2016). In surviving plants, PLC from water stress and/or freezing stress typically recovers by the formation of new conduits in xylem (Sperry et al. 1994) or refilling of embolized conduits in some species such as grapevine (Brodersen et al. 2010).

Vulnerability curves (VCs) show the relationship of PLC with increasingly negative pressure (Sperry et al. 1988, Pammenter and Vander Willigen 1998, Choat et al. 2016). Stem VCs can change through the season, with branch age and in response to prior drought (Sperry and Sullivan 1992, Kolb and Sperry 1999, Domec et al. 2006). Stem VCs can also differ within individuals (Sperry and Saliendra 1994) and within branches of a single tree (Domec et al. 2008). The cause of this variation is unknown but probably involves a combination of xylem development and ageing effects on inter-conduit pit membrane function (Sperry et al. 1991, Melcher et al. 2003, Choat et al. 2008). The 'cavitation fatigue' phenomenon, for example, refers to increases in vulnerability associated with previous cavitation and refilling cycles, and may result from weakening the ability of pit membranes to prevent the air-seeding of cavitation (Hacke et al. 2001, Hillabrand et al. 2016). Age-related increases in vulnerability

may also contribute, along with increased shading, to the senescence and dieback of older, lower branches in tree crowns.

In this paper, we investigate the possibility of 'pressure fatigue': an increase in vulnerability to cavitation associated with the cycling of pressures that are not extreme enough to induce significant cavitation. Pressure cycling will repeatedly stress inter-conduit pit membranes between water-filled and embolized conduits. These membranes are the potential sites for the air-seeding of cavitation. As the conduit ages, the number of such daily pressure cycles increases, and the cumulative stress on inter-conduit pit membranes could reduce their air-seeding pressure and alter the branch VC. Ultimately, cavitation could result even without any change in the magnitude of the sap pressure.

Previous cycle effects have been seen using the 'static' centrifuge method, but these were shown to be artifacts caused by drying of branch ends between spins (Tobin et al. 2013). Our experiments avoided this artifact by keeping branch ends submerged at all times. In addition, we distinguished between effects of cycling vs cumulative exposure time to negative pressure. Where possible we assessed effects of cycling within single stem samples to avoid confounding effects of differences between stems. We assessed the effect of pressure cycles at two branch positions: upper crown and lower crown. The study species was *Acer negundo* L., a common semi-riparian tree. This species was previously found to not experience cavitation fatigue, evidenced from no change in branch VC following artificial refilling of embolism (Hacke et al. 2001). To minimize artifacts, we assessed the cycling effect with three techniques: the 'static' centrifuge method (no flow during spinning), the 'flow' centrifuge method (flow during spinning) and air-injection (cycling air pressure rather than sap pressure).

Materials and methods

Plant materials

All branch segments of young *A. negundo* trees were collected from natural populations growing at a single site in the Red Butte Canyon Research Natural Area (~15 km east of the University of Utah) (40.779010 N, 111.811894 W). Tree height ranged from 5 to 8 m, and diameter at breast height ranged from 4 to 7 cm. The xylem pressure was measured using pressure chamber (PMS Instrument Company, Albany, OR, USA) to define the maximal and the minimal xylem pressures on clear, sunny days during summer season of the experimental years (June to August in 2013 and 2014). Leaves were bagged for at least 30 min to equilibrate with branches before their removal from the plant. Three leaves each from upper and lower branches were used to obtain mean midday and predawn stem xylem pressures. Pressures were measured five times per experimental year. 'Upper' branches were collected from the sun-exposed top of the crown. 'Lower' branches were collected from the bottom extremity of the crown, but still exposed to sun because the

trees were growing in the open (see Figure S1 available as Supplementary Data at *Tree Physiology* Online). Collected branches were ~50 cm in length and were from 8 to 15 mm in basal diameter. Sampled branches were immediately wrapped tightly in plastic bags (humidified with damp towels) and brought to our laboratory.

All branches were used within 3 days of harvesting. In the laboratory, 150 or 280 mm length segments were excised under water. Upper branches were generally 3 years old, and lower branches were usually 7 years old. Bark of both branch ends was peeled except for segments used for the air-injection method. Before the K_h measurement, samples ends were trimmed with a fresh razor blade until the branch length was ~145, 270 or 275 mm, and all samples were flushed with filtered (0.2 μm) 20 mM KCl solution for 30 min at ~75 kPa to remove pre-existing air emboli.

Centrifuge vulnerability curves

Vulnerability curves ($n = 5$ branch segments) were made for upper and lower branches using the static centrifuge method. All samples were ~275 mm in length, and basal diameters were 10.6 ± 1.1 mm (mean $\pm$ standard deviation) in upper branches and 9.8 ± 1.3 mm in lower branches.

After all segments were flushed to reverse any native embolism, they were pre-spun in a rotor for 5 min at −0.1 MPa (Sorvall RC-5C; Thermo Fisher Scientific, Waltham, MA, USA). Branch ends were submersed in water in Plexiglas reservoirs during spinning (Alder et al. 1997). After this pre-spin, segments were immediately attached to a tubing apparatus filled with the same 20 mM KCl solution for measuring the initial hydraulic conductivity, $K_{h\,initial}$. The $K_{h\,initial}$ was calculated from net pressure-driven flow (corrected for background flow; Hacke et al. 2000, Torres-Ruiz et al. 2012) divided by the pressure gradient (induced by 4–6 kPa hydraulic head).

After the measurement of $K_{h\,initial}$, the centrifuging process was repeated at progressively more negative pressures until −4.0 MPa where K_h approached zero. Vulnerability curves were analyzed as PLC.

Cycle effects induced by flow centrifuge method

We used the flow centrifuge method (Cochard et al. 2005) as implemented by Li et al. (2008). All samples ($n = 20$) were ~275 mm in length, and basal diameters were 9.5 ± 1.1 mm in upper branches ($n = 10$) and 9.6 ± 1.2 mm in lower branches ($n = 10$). Upper and lower branches ($n = 5$) were used to assess the change in K_h with 10 pressure cycles between −0.5 MPa (for 5 s) and −2.0 MPa (for 5 min) (i.e., representing the maximal and minimal xylem pressures on clear summer days). Prior to this pressure cycling, flushed samples were spun for 5 min at −0.5 MPa and then $K_{h\,initial}$ was measured at −0.5 MPa as described in Li et al. (2008). After each 5 min cycle at −2.0 MPa, K_h was measured again (see Figure S2a

available as Supplementary Data at *Tree Physiology* Online). Thus, stems were not removed and ends remained immersed in KCl solution for the entire cycling. To distinguish effects of cycling vs time at −2.0 MPa, a set of control branches ($n = 5$) were spun for 50 min at −2.0 MPa, giving the same period of exposure to −2 MPa but without cycling. K_h was measured at the same time intervals as above.

Cycle effects induced by static centrifuge method

The static method was the same as described for obtaining the full VC. All samples ($n = 50$) were ~145 mm in length, and basal diameters were 10.0 ± 0.9 mm in upper branches ($n = 25$) and 9.9 ± 1.1 mm in lower branches ($n = 25$). Upper and lower branches ($n = 5$) were used to detect cycle effects of 10 or 20 cycles between −0.5 MPa (5 s) and −2.0 MPa (see Figure S2b available as Supplementary Data at *Tree Physiology* Online). For the 10 cycle treatment, branches were held 5 min at −2.0 MPa (total of 50 min); for 20 cycle treatment, branches were held 2 min at −2.0 MPa (total of 40 min). A set of controls were spun at −2.0 MPa for 50 min continuously, and then at −0.5 MPa continuously for 10 min, to compare effects of cumulative time at pressure without any cycling (see Figure S2b available as Supplementary Data at *Tree Physiology* Online). After the initial flush, samples were secured in the rotor, and all samples were spun for 5 min at −0.5 MPa. After this initial centrifuging, segments were immediately attached to the tubing apparatus filled with the 20 mM KCl solution for measuring $K_{h\,initial}$. After the measurement of $K_{h\,initial}$, the branch was centrifuged through its pressure regime (10 or 20 cycle) without stopping the centrifuge (thus keeping the branch ends submerged). At the end of the period, each stem was attached to the tubing apparatus and K_h was measured again.

As additional controls, after the measurement of $K_{h\,initial}$, we determined the PLC after a single spin for 5 min at −2.0 MPa, or a spin of 60 min at −0.5 MPa. We also determined the effect of simply soaking branches in water for the same cumulative time (60 min) with no spinning after the measurement of $K_{h\,initial}$.

Cycle effects induced by single-ended air injection

All branches were ~270 mm in length (basal diameter = ~9 mm). After an initial flush, air was injected at 0.1 MPa (for 5 min) from the basal end. The $K_{h\,initial}$ was measured on a segment of 55 mm length cut underwater from the distal end of the air-injected sample. Distal segment diameters were 6.9 ± 1.1 mm in upper branches ($n = 20$) and 7.3 ± 1.1 mm in lower branches ($n = 20$). Five sample branches were used per each treatment. The K_h measurement used the same tubing apparatus and protocol used for the static centrifuge experiments. The remaining branch was then injected (from the same basal end) with air cycling between 0.5 MPa (5 s) and 2.0 MPa for 10 or 20 times. The 10-cycled branches were held at 2.0 MPa for 5 min, 20-cycled branches were held for 2 min. Non-cycled

branches were injected at 0.5 MPa for 10 min and at 2.0 MPa for 50 min. After the pressure cycling, a second segment of 55 mm length was cut (underwater) from the distal end of the air-injected sample and K_h was measured after bubbles ceased to emit from the either end of the branch (generally >2 h).

As a control, air was injected basally at 0.1 MPa (for 5 min), two 55 mm segments were cut from the distal end, soaked for the same time as the high-pressure branches, and K_h of the 55 mm segments measured.

Vessel diameters

Vessel measurements were conducted for upper and lower branches. The sample diameter was 10.7 ± 0.3 mm in upper branches ($n = 4$) and 9.5 ± 0.6 mm in lower branches ($n = 4$). Cross sections of 20–30 μm thickness were taken with a sliding microtome (LS-113, Yamato kohki, Saitama, Japan). We obtained images of the sections using a digital camera attached to a light microscope, and the images were imported into the ImageJ version 1.52 (http://imagej.nih.gov/ij/) for analysis. We defined a radial sector spanning the initial and terminal borders of the current-year's annual ring, enclosing 100 or more vessels, and all vessels in the radial sector were measured. The hydraulic diameter (D) of the lumen was calculated as $D = \sqrt{(xy)}$, where x and y were the major and minor axis diameter of the vessel, respectively. We measured mean hydraulic vessel diameters, which was defined as $[(\Sigma D^4)/N]^{1/4}$, where N was the number of vessels (Tyree and Zimmermann 2002).

Statistics

Pair–wise comparisons of means were made with *t*-tests. Comparisons between three or more means employed ANOVA using R software (version 3.4.1; R Development Core Team 2017), followed by post-hoc Tukey HSD test to determine differences between particular means or groups of means.

Results

Upper vs lower branch vulnerability curves, negative xylem pressures and vessel diameters

Branches from the upper crown (generally 3 years old) had significantly greater $K_{h\,initial}$ (by a factor of 1.7; Figure 1a) and were more resistant to cavitation (Figure 1b) than branches from the lower crown (generally 7 years old). The VCs (static centrifuge method) showed a P_{50} for upper branches of −2.44 MPa vs −2.16 MPa for lower branches. The PLC at −2.0 MPa was also less in upper [21.2 ± 11.8 (mean ± stand deviation)%] vs lower branches ($38.3 \pm 22.3\%$; Figure 1b), although the trend was not statistically significant. Stem xylem pressure showed $−0.30 \pm 0.04$ MPa at predawn vs $−2.15 \pm 0.09$ MPa at midday, with no trend in upper and lower branches through the growing season. Thus, lower branches had lower inherent conducting capacity and were more vulnerable to embolism than upper ones.

(a)

(b)
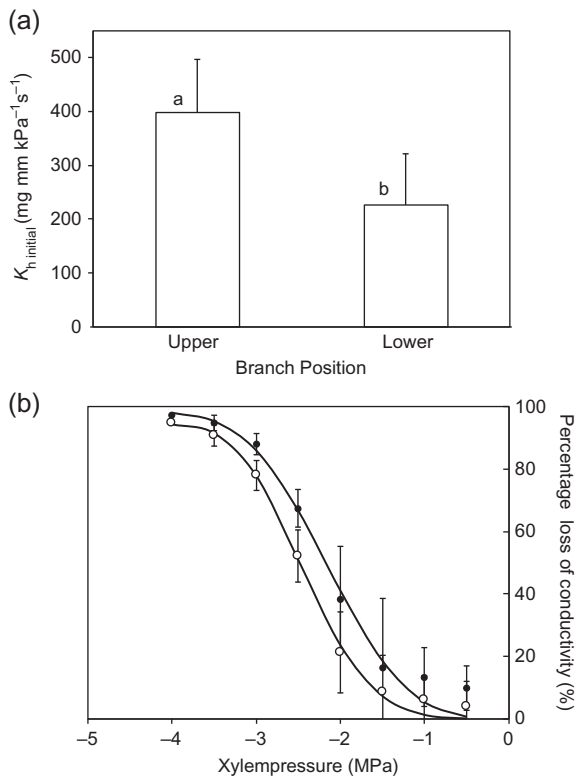
Figure 1. (a) Initial hydraulic conductivity ($K_{\text{h initial}}$) of upper vs lower branches in *Acer negundo*. Different letters indicate a significant difference between branch positions (*t*-test, $P = 0.05$). (b) Vulnerability curves from the static centrifuge method in *A. negundo*. Conductive capacity for vulnerability curves is expressed as the percentage loss of conductivity relative to the initial conductivity value in (a). Open and closed symbols showed vulnerability curves for upper and lower branches, respectively. Error bars are ± 1 SD for $n = 5$ samples. Data are fit with a Weibull function.

(a)

(b)

Figure 2. (a) Initial percentage loss of conductivity (PLC) at −2.0 MPa as measured by the flow centrifuge method on segments collected from upper vs lower branch positions ($n = 10$ per position). Different letters indicate significance (*t*-test, $P = 0.05$ cutoff). (b) The difference in PLC from initial value in (a) for samples continuously spinning at −2.0 MPa (triangles) vs samples repeatedly cycled from −0.5 to −2.0 MPa (circles) ($n = 5$). Open and closed symbols show the data from the upper and lower branches, respectively. Error bars are ±1 SD. Different letters above the last reading at 50 min indicates significant difference among treatments by a post-hoc Tukey HSD test ($P = 0.05$).

Mean hydraulic vessel diameter in the current-year xylem of upper branches ($35.5 \pm 1.4\,\mu\text{m}$) was wider than that of lower branches ($27.5 \pm 2.9\,\mu\text{m}$). The vessel diameter values of both branches were statistically different (*t*-test, $P = 0.002$).

Cycle effects induced by flow centrifugation

When spun once for 5 min at −2 MPa, upper branches had lower PLC ($17.0 \pm 5.6\%$) than lower ones ($33.5 \pm 12.9\%$; Figure 2a). This result was consistent with the PLC at −2.0 MPa for the VCs generated with the static method (Figure 1b). Subsequent cycling of pressure between −2.0 MPa and −0.5 MPa caused a significant further increase in PLC (by $19.9 \pm 9.1\%$ after 10 cycles for a total PLC of ~51%) in lower branches (Figure 2b, closed circles). The additional PLC resulted from cycling rather than cumulative exposure to −2.0 MPa, because lower branches held continuously at −2.0 MPa showed no further increase in PLC (Figure 2b, closed triangles). In contrast, upper branches showed no increase in PLC either by cycling or continuous exposure to −2.0 MPa (Figure 2b, open symbols).

Cycle effects induced by static centrifugation

The PLC caused by 5 min at −2.0 MPa for static centrifugation was similar to that seen for the flow method, with upper branches having less PLC than lower ones (Figure 3a). However, 50 min at −2.0 MPa caused a significant increase in upper branch PLC with the static method (Figure 3a) vs no increase observed in the flow method (Figure 2b). Lower branch PLC showed no significant increase from 5 to 50 min of continuous exposure to −2.0 MPa with either method (Figures 2b and 3a).

The effect of pressure cycling (between −2.0 and −0.5 MPa) with the static method was very similar to that observed with the flow method. Lower branches increased their PLC in response to 10 (PLC = $60.1 \pm 13.0\%$) or 20 (PLC = $68.6 \pm 8.8\%$) cycles, and upper branches showed no cycle response (Figure 3b). Control branches showed less than 7.2 ± 3.4 PLC in response to either soaking for 50 min or spinning at −0.5 MPa for 50 min suggesting no effect of time for the centrifuge environment.
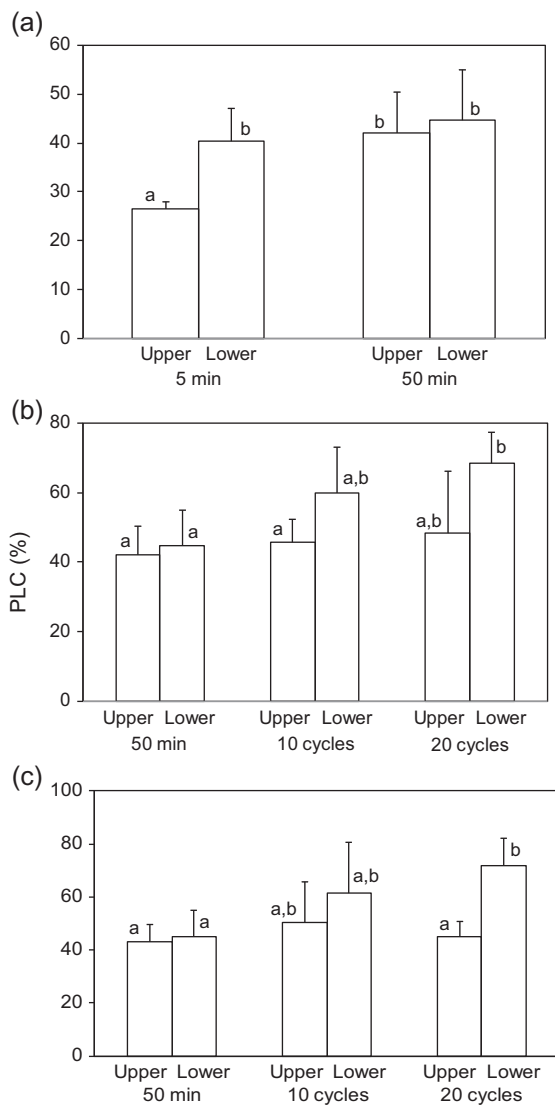
Figure 3. (a) The percentage loss of hydraulic conductivity (PLC) from the static centrifuge method after a single spin for 5 min vs 50 min at −2.0 MPa for upper and lower branches. (b) The PLC from the static centrifuge method for samples kept at −2.0 MPa for 50 min vs samples cycled between −0.5 and −2.0 MPa 10 or 20 times over 50 min. (c) The PLC for segments air-injected at 2.0 MPa for 50 min vs samples cycled between 0.5 and 2.0 MPa of air pressure for 10 or 20 times over 50 min. Error bars are ± 1 SD, $n = 5$, different letters above the columns indicate significant differences by post-hoc Tukey HSD test ($P = 0.05$).

Cycle effects induced by single-ended air injection

Air injection produced nearly identical results as static centrifugation. The PLC after 50 min at 2.0 MPa was similar between upper and lower branches (Figure 3c), and similar to that caused by static centrifugation (Figure 3b). Lower branches increased their PLC in response to 10 (PLC = 61.4 ± 19.3%) or 20 (PLC = 71.9 ± 10.1%) cycles, and upper branches showed no cycle response (Figure 3c). Control branches injected at 0.1 MPa showed less than 25.6 ± 18.0 PLC, indicating that the excised K_h segments were far enough removed from the air injection point to avoid embolism via air-filling of continuous vessels.

Discussion

The results provided strong evidence that pressure cycles selectively increase the vulnerability to cavitation in lower crown branches of *A. negundo*. All methods agreed in showing a similar PLC increase and K_h decrease (see Figure S3 available as Supplementary Data at *Tree Physiology* Online) associated with 10 or 20 pressure cycles in branches from the lower crown. The agreement between diverse methods and the various control experiments rules out a role for the branch drying artifact identified by Tobin et al. (2013). The results confirm the effect of cycling itself, as opposed to cumulative exposure to stress. Twenty cycles caused the PLC to reach around 70% for lower branches (Figure 3b and c). Drought mortality in angiosperms has been associated with 88% loss of conductivity (P_{88}) (Urli et al. 2013). In our experiment, $K_{h \text{ inital}}$ of lower branches was already lower than upper ones (Figure 1a and Figure S3 available as Supplementary Data at *Tree Physiology* Online), consistent with their narrower vessel diameter. The greater vulnerability of lower branches to pressure fatigue would tend to exacerbate the limited flow capacity of lower branches.

The fact that air pressure cycles produced very similar results to sap pressure cycles implies that mechanical stress is involved rather than fluid pressure per se. A likely candidate is mechanical fatigue of inter-vessel pit membranes. Membranes between sap- and air-filled conduits would be repeatedly flexed as either sap- or air-pressure was cycled. Flexing could weaken the pit membranes, induce membrane creep and increase porosity. Stressed membranes could ultimately allow cavitation to arise even without drop in minimum negative pressure. The weakening of pit membranes is also the proposed mechanism for 'cavitation fatigue', which is observed after successive cavitation and refilling cycles (Hacke et al. 2001). In the present case, however, the fatigue is induced by pressure cycling without intervening refilling of conduits. If this interpretation is correct, branches from the upper crown must produce more perfectly elastic pit membranes than lower branches, perhaps because of a better growth environment in the upper crown. It seems likely that growth environment and branch age are critical, because segments measured were themselves of different age and necessarily included the current year's growth ring. The implication is that what may be subtle differences in pit membrane chemistry and structure could have large functional consequences. This suggests there could also be variation in cavitation fatigue (weakening associated with cavitation and refilling cycles; Hacke et al. 2001) depending on branch position in a single tree. If so, the immunity of some *A. negundo* branches to cavitation fatigue (Hacke et al. 2001) may not be true at all positions in the crown. More work needs to be done to understand the role of pit membrane mechanics on air seeding pressures (Sperry and Tyree 1990).

It is not clear what caused the increase in PLC from 5 to 50 min spin time for the upper branch segments with the static

centrifuge method. Lower branch segments also showed an increase, though it was not significant. There was no corresponding time effect for flow centrifugation. Previous experiments with the static method have either shown no effect of centrifuge time (Alder et al. 1997 in *Betula occidentalis*), or have attributed an observed PLC increase as an artifact of branch dehydration when the solution-filled reservoirs that are intended to cover the branch ends are depleted by evaporation (Tobin et al. 2013). In the flow method, these reservoirs are kept full during flow measurements. Regardless, in all experiments there was a clear increase in PLC of lower branches that was associated with pressure cycling, over and above the effect of cumulative exposure time.

The impact of the pressure fatigue we observed in the laboratory on in vivo hydraulics remains to be seen. The minute-scale pressure cycles induced in the centrifuge or with air injection are far shorter than the hours-long diurnal cycles in the intact plant. Nevertheless, the results warrant further investigation, because they could help explain not only senescence-related declines in branch vigor, but observed shifts to more vulnerable xylem seen in larger trees (Rowland et al. 2015) and trees weakened from exposure to prior drought (Anderegg et al. 2015).

Supplementary Data

Supplementary Data for this article are available at *Tree Physiology* Online.

Conflict of interest

None declared.

Funding

References

Alder NN, Sperry JS, Pockman WT (1996) Root and stem xylem embolism, stomatal conductance, and leaf turgor in *Acer grandidentatum* along a soil moisture gradient. Oecologia 105:293–301.

Alder NN, Pockman WT, Sperry JS, Nuismer S (1997) Use of centrifugal force in the study of xylem cavitation. J Exp Bot 48:665–674.

Anderegg WRL, Schwalm C, Biondi F et al. (2015) Pervasive drought legacies in forest ecosystems and their implications for carbon cycle models. Science 349:528–532.

Barigah ST, Charrier O, Douris M, Bonhomme M, Herbette S, Améglio T, Fichot R, Brignolas F, Cochard H (2013) Water stress-induced xylem hydraulic failure is a causal factor of tree mortality in beech and poplar. Ann Bot 112:1431–1437.

Brodersen CR, McElrone AJ, Choat B, Matthews MA, Shackel KA (2010) The dynamics of embolism repair in xylem: In vivo visualizations using high-resolution computed tomography. Plant Physiol 154:1088–1095.

Choat B, Cobb AR, Jansen S (2008) Structure and function of bordered pits: new discoveries and impacts on whole-plant hydraulic function. New Phytol 177:608–626.

Choat B, Badel E, Burlett R, Delzon S, Cochard H, Jansen S (2016) Noninvasive measurement of vulnerability to drought-induced embolism by X-ray microtomography. Plant Physiol 170:273–282.

Cochard H, Tyree MT (1990) Xylem dysfunction in *Quercus*: vessel sizes, tyloses, cavitation and seasonal changes in embolism. Tree Physiol 6:393–407.

Cochard H, Damour G, Bodet C, Tharwat I, Poirier M, Améglio T (2005) Evaluation of a new centrifuge technique for rapid generation of xylem vulnerability curves. Physiol Plant 124:410–418.

Davis SD, Sperry JS, Hacke UG (1999) The relationship between xylem conduit diameter and cavitation caused by freezing. Am J Bot 86:1367–1372.

Domec JC, Lachenbruch B, Meinzer FC (2006) Bordered pit structure and function determine spatial patterns of air-seeding thresholds in xylem of douglas-fir (*Pseudotsuga menziesii*; Pinaceae) trees. Am J Bot 93:1588–1600.

Domec JC, Lachenbruch B, Meinzer FC, Woodruff DR, Warren JM, McCulloh KA (2008) Maximum height in a conifer is associated with conflicting requirements for xylem design. Proc Natl Acad Sci USA 105:12069–12074.

Hacke UG, Sperry JS, Pittermann J (2000) Drought experience and cavitation resistance in six shrubs from the Great Basin, Utah. Basic Appl Ecol 1:31–41.

Hacke UG, Stiller V, Sperry JS, Pittermann J, McCulloh KA (2001) Cavitation fatigue. Embolism and refilling cycles can weaken the cavitation resistance of xylem. Plant Physiol 125:779–786.

Hillabrand RM, Hacke UG, Lieffers VJ (2016) Drought-induced xylem pit membrane damage in aspen and balsam poplar. Plant Cell Environ 39:2210–2220.

Kolb KJ, Sperry JS (1999) Transport constraints on water use by the Great Basin shrub, *Artemisia tridentata*. Plant Cell Environ 22:925–935.

Li S, Feifel M, Karimi Z, Schuldt B, Choat B, Jansen S (2016) Leaf gas exchange performance and the lethal water potential of five European species during drought. Tree Physiol 36:179–192.

Li Y, Sperry JS, Taneda H, Bush SE, Hacke UG (2008) Evaluation of centrifugal methods for measuring xylem cavitation in conifers, diffuse- and ring-porous angiosperms. New Phytol 177:558–568.

Melcher PJ, Zwieniecki MA, Holbrook NM (2003) Vulnerability of xylem vessels to cavitation in sugar maple. scaling from individual vessels to whole branches. Plant Physiol 131:1775–1780.

Pammenter NW, Vander Willigen C (1998) A mathematical and statistical analysis of the curves illustrating vulnerability of xylem to cavitation. Tree Physiol 18:589–593.

Rowland L, da Costa ACL, Galbraith DR et al. (2015) Death from drought in tropical forests is triggered by hydraulics not carbon starvation. Nature 528:119–122.

Sperry JS, Saliendra NZ (1994) Intra- and inter-plant variation in xylem cavitation in *Betula occidentalis*. Plant Cell Environ 17:1233–1241.

Sperry JS, Sullivan JEM (1992) Xylem embolism in response to freeze-thaw cycles and water stress in ring-porous, diffuse-porous, and conifer species. Plant Physiol 100:605–613.

Sperry JS, Tyree MT (1990) Water-stress-induced xylem embolism in three species of conifers. Plant Cell Environ 13:427–436.

Sperry JS, Tyree MT, Donnelly JR (1988) Vulnerability of xylem to embolism in a mangrove vs an inland species of Rhizophoraceae. Physiol Plant 74:276–283.

Sperry JS, Perry AH, Sullivan JEM (1991) Pit membrane degradation and air-embolism formation in aging xylem vessels of *Populus tremuloides* Michx. J Exp Bot 42:1399–1406.

Sperry JS, Nichols KL, Sullivan JEM, Eastlack SE (1994) Xylem embolism in ring-porous, diffuse-porous, and coniferous trees of Northern Utah and Interior Alaska. Ecology 75:1736–1752.

Tobin MF, Pratt RB, Jacobsen AL, De Guzman ME (2013) Xylem vulnerability to cavitation can be accurately characterised in species with long vessels using a centrifuge method. Plant Biol 15:496–504.

Torres-Ruiz JM, Sperry JS, Fernández JE (2012) Improving xylem hydraulic conductivity measurements by correcting the error caused by passive water uptake. Physiol Plant 146:129–135.

Tyree MT, Zimmermann MH (2002) Xylem structure and the ascent of sap. Springer, Berlin.

Umebayashi T, Morita T, Utsumi Y, Kusumoto D, Yasuda Y, Haishi T, Fukuda K (2016) Spatial distribution of xylem embolisms in the stems of *Pinus thunbergii* at the threshold of fatal drought stress. Tree Physiol 36:1210–1218.

Urli M, Porté AJ, Cochard H, Guengant Y, Burlett R, Delzon S (2013) Xylem embolism threshold for catastrophic hydraulic failure in angiosperm trees. Tree Physiol 33:672–683.